

# Design and Performance Analysis of a Metamorphic Mechanism with Constrained Joint



Qiang Yang, Xin Zhao, Ruonan Wang, Hailong Huang, Shujun Li, and Benqi Sun

**Abstract** The structural design of constrained joints is an effective way to realize the type synthesis of constrained metamorphic mechanism. In previous studies, constrained joints are often represented in the form of kinematic diagrams of mechanism, which doesn't provide enough reference to the practical application of metamorphic mechanisms. On the basis of summarizing the constraint forms and resistance characteristics of the commonly used variable-constraint constrained joints, and according to the force analysis of the augmented Assur group with constrained joints, a new constrained revolute joint with combined variable-constraint of spring force and geometric constraint is designed, which has advantages such as simple structure, reliable working ability and passive adaptive capability to operational conditions. Based on this constrained joint, a two-configuration constrained metamorphic mechanism with under-actuated is designed, the force analysis of the mechanism is completed, and the effectiveness and feasibility of design approach proposed in this paper is verified for the constraint parameters of the invented metamorphic joint. The novel combinatorial variable-stiffness constrained joint can obtain stable and reliable configuration switching ability, which provides a feasible way for promoting the engineering application of metamorphic mechanism.

**Keywords** Constrained metamorphic mechanism · Constrained joint · Variable-constraint · Structure of constrained joint · Force analysis

---

Q. Yang (✉) · X. Zhao · R. Wang · S. Li · B. Sun  
College of Mechanical Engineering and Automation, Northeastern University, Shenyang 110819, China  
e-mail: [qiangyang@mail.neu.edu.cn](mailto:qiangyang@mail.neu.edu.cn)

Q. Yang · X. Zhao  
Key Laboratory of Lifting Equipment's Safety Technology for State Market Regulation, Liaoning Inspection, Examination and Certification Centre, Shenyang 110036, China

Q. Yang · H. Huang  
College of Mechanical Engineering and Automation, Liaoning University of Technology, Jinzhou 121001, China  
e-mail: [jxhuanghl@lnut.edu.cn](mailto:jxhuanghl@lnut.edu.cn)

## 1 Introduction

At the 25th Biennial Mechanisms and Robotics Conference (ASME) in 1998, Dai et al. [1] first proposed the concept of metamorphic mechanisms. Li et al. [2] proposed a structure synthesis method of metamorphic mechanisms based on the matrix operation of configuration transformation. Dai et al. [3] systematically introduced metamorphic ways and a general categorization of metamorphic mechanisms. Wang et al. [4] established the metamorphic equation of metamorphic mechanisms on the basis of exploring the composition and expression of metamorphic mechanisms. Li et al. [5] presented the concept of augmented Assur groups and the structure composition of single-driven metamorphic mechanisms based on augmented Assur groups. Zhang et al. [6] proposed a method for configuration synthesis of metamorphic mechanisms based on constraint variation. Yang et al. [7] proposed a general structural design method of a planar metamorphic mechanisms based on the structural synthesis matrix. Gan et al. [8] designed a new reconfigurable rT Hooke's joint and proposed two types of metamorphic parallel mechanisms based on it. Zhang et al. [9] designed a new variable-axis (vA) joint, which realized the switching of revolute joint, Hooke's joint and spherical joint. Zhao et al. [10] presented a new lockable spherical (lS) joint, which can realize the switch between Hooke and spherical joint. Wang et al. [11] presented a novel reconfigurable spherical (rS) joint, which can realize the switch between revolute and spherical joint. Liu et al. [12] summarized the design catalogues of variable constraint joints to design the variable topology mechanism. YAN and KUO studied the topological representations and characteristic analysis of variable kinematic joints [13]. Li et al. [14] first proposed a new method for the constraint force analysis of metamorphic joints. Yang et al. [13] studied the type synthesis of constrained metamorphic mechanisms with structural forms of metamorphic joints. The metamorphic of kinematic joints is one of the key methods to synthesize the new configuration of metamorphic mechanisms [4]. Changing the type of the kinematic joint [9–11] and constraining the kinematic status of the kinematic joint are two common methods to realize the configuration transformation of the kinematic joint. Among them, the multi-configurations metamorphic mechanism operated in an under-actuated state was proposed using the latter metamorphic method. The ability of obtaining convenient variable-working configuration/variable-topological structure is the key performance of metamorphic mechanism for practical application. The constrained metamorphic mechanism realizes the transforming/keeping of working configurations by the transforming/keeping of the moving and static of the metamorphic joints (variable kinematic joints). Therefore, some specific “switch” structures of metamorphic joints need to be designed for realizing the transforming between moving and static, and then obtain the ideal variable constraint form and constraint characteristics of the metamorphic joint to obtain the stability and reliability of the configuration transformation of constrained metamorphic mechanisms.

## **2 The Constraint Forms and Resistance Characteristics of the Common Variable-Constraint Constrained Joints**

The main realization forms of the variable constraint metamorphic joints include: constraints provided by the structure of metamorphic joints that include geometric constraints (geometric limitations), force constraints (spring force, gravity, reaction force, etc.) and the constraints provided by the structural parameters of the mechanism on metamorphic joints, etc. Some typical constraint forms and constraint characteristics include: Geometric constraint: geometric limitation, or lock/unlock the limit controlled by profiles of links and/or joints (e.g., cam). The geometric constraint could theoretically provide infinite constraint force. Force constraint: spring force constraint or geometric constraint controlled by spring, which provides variable constraint force. The magnitude of the force is determined by the spring force and practical structure, which are easily adjusted. Combined constraint: combined arrangements of geometric and force constraints.

Several typical variable constraint metamorphic joints are shown in Figs. 1, 2, 3, 4 and 5. Figure 1 shows metamorphic joints with a geometric constraint, which provides infinite force at the limit position. Figures 2 and 3 respectively show metamorphic joints with spring force constraint and geometric constraint controlled by spring force, which provide the constraint force controlled by the geometric profile and spring force at the limit position. Figure 4 shows metamorphic joints with spring force and geometric constraints. Finally, metamorphic joints with geometric constraint and geometric constraint controlled by spring force are shown in Fig. 5. The corresponding constraint force characteristic sketches are also given in the above figures.

## **3 The Force Analysis and Structure Design of the Metamorphic Revolute Joint with Combined Variable-Constraint of Spring Force and Geometric Constraints**

Because of its simple structure, reliable operation and strong adaptability, the metamorphic revolute joint shown in Fig. 4a with spring force and geometric constraints is considered to be successfully employed in many industrial fields. However, in previous study, the variable constraint metamorphic joints is often drawn in kinematic diagram without structure design. For practical application, designing the structure of the metamorphic revolute joint is an essential link, and completing the force analysis of the metamorphic revolute joint is the premise of its structural design. A typical application case is shown in Fig. 6. In Fig. 6a, the revolute joint 2 is a metamorphic revolute joint with spring force and geometric constraints, and the prismatic joint 4 is a metamorphic prismatic joint with geometric constraint. In the process of configuration transformation, the RRRP augmented Assur group (AAG) [5] degenerates into

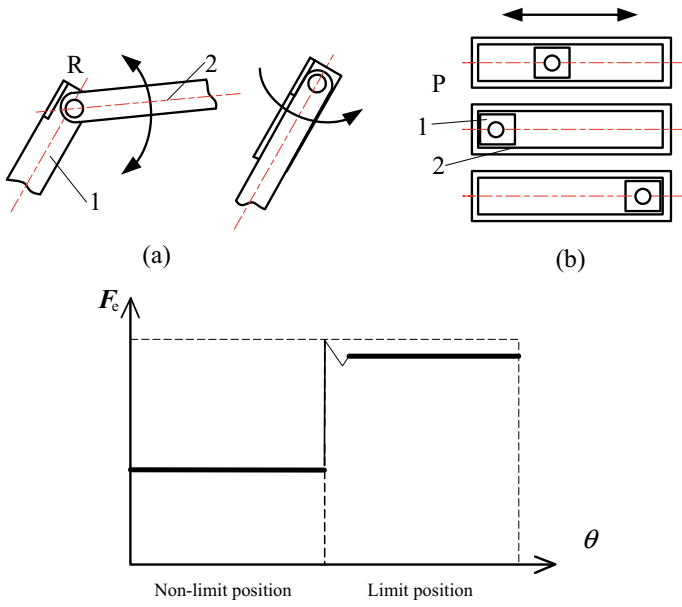


**Fig. 1** Metamorphic joints constrained by geometric limitation

**Fig. 2** Metamorphic joints constrained by spring force regulation

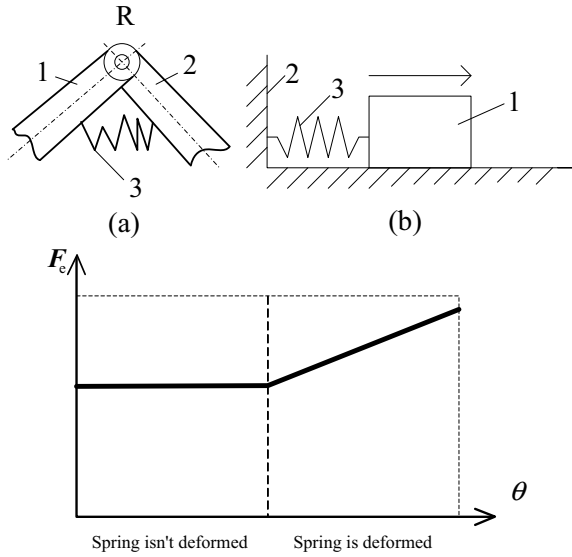
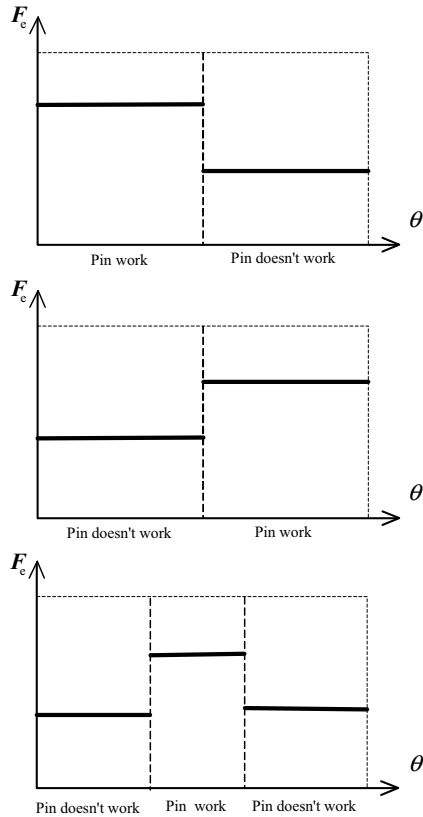
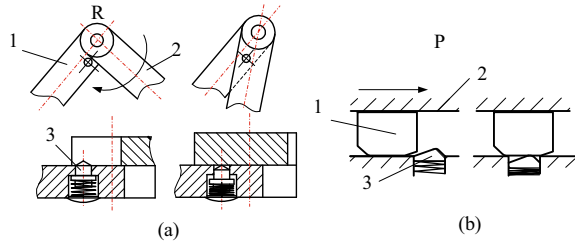
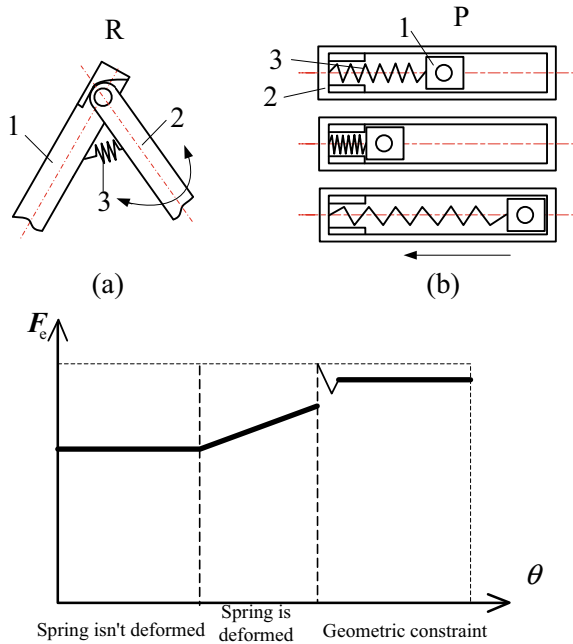


**Fig. 3** Metamorphic joints with geometric constraint controlled by spring



RRP and RRR equivalent Assur groups (AGs) in turn. In the working configuration I, link 1 and link 2 are annexed into a united one because metamorphic revolute joint 2 is constrained to keep static, and the metamorphic prismatic joint 4 moves simultaneously, so the AAG RRRP degenerates into the RRP group (Fig. 6b). In the working configuration II, the metamorphic prismatic joint 4 is constrained to transform from moving to static, the metamorphic revolute joint 2 changes from static to moving, so the AAG RRRP degenerates into the RRR group (Fig. 6c).

**Fig. 4** Metamorphic joints constrained by geometric and spring force constraints

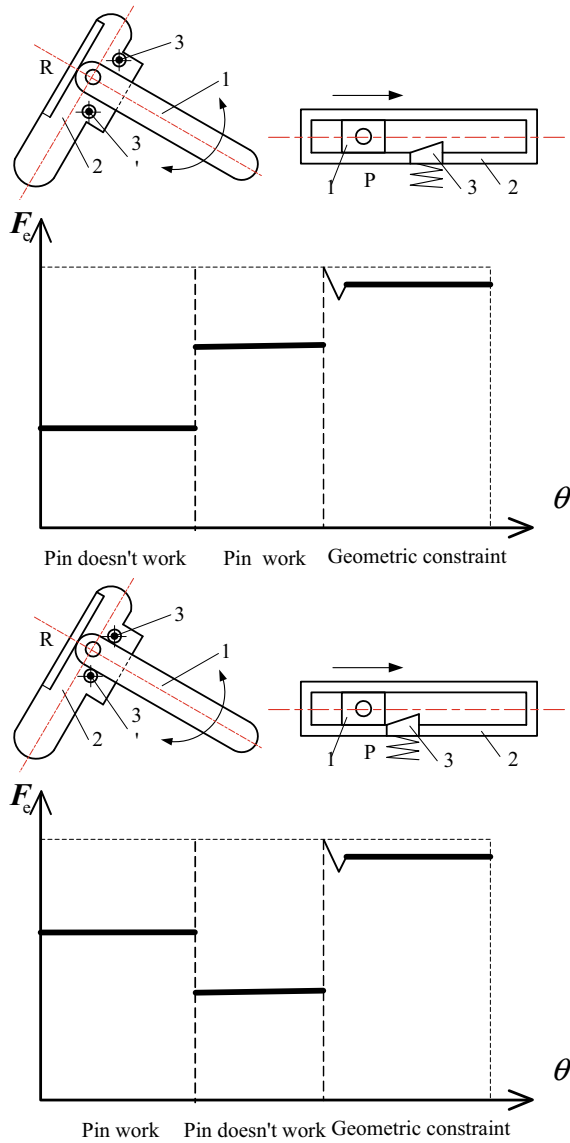


When the metamorphic joint is in the constraint status (static), the AAG will degenerate into the corresponding equivalent AG, so the kinematic analysis method of the AAG [15] is nearly the same as that of the corresponding AG. Due to the existence of geometric and spring force constraints, the calculation of constraint force (torque) in the metamorphic revolute joint is very important, and it is also the basis of its structural design. Therefore, based on the conventional force analysis method of AG and combined with the configuration transformation process of RRRP group, a force analysis model of the metamorphic revolute joint with spring force and geometric constraints is established.

### 3.1 Force Analysis of the Metamorphic Revolute Joint

In the working configuration I, the AAG RRRP degenerates into the AG RRP. The force analysis of the corresponding equivalent AG RRP is shown in Fig. 7, where points  $N_4$ ,  $N_5$  and  $N_6$  are the centroids of the links  $N_1N_2$ ,  $N_2N_3$  and the slider respectively (the centers of mass are determined under assumption),  $l_{12}$ ,  $l_{23}$  and  $l_{13}$  represent the lengths of  $N_1N_2$ ,  $N_2N_3$  and  $N_1N_3$  respectively, and  $F_\beta$  is the component of the external force acted on the slide along the moving direction. Suppose that the external forces  $F_4$ ,  $F_5$ ,  $F_6$  and moments  $T_1$ ,  $T_2$ ,  $T_3$  acted on the links  $N_1N_2$ ,  $N_2N_3$

**Fig. 5** Metamorphic joints with geometric constraint and geometric constraint and geometric constraint controlled by spring force



and the slider respectively are known, solve the reaction force of each revolute joint and the driving torque and constraint torque of the metamorphic revolute joint.

Modularized force analysis procedures are as follows:

$$\cos \alpha = \frac{l_{12}^2 + l_{23}^2 - l_{13}^2}{2l_{12}l_{23}} = \frac{d_1^2 + d_2^2 - d_k^2}{2d_1d_2} \quad (1)$$

**Fig. 6** Configuration transformation process of RRRP group

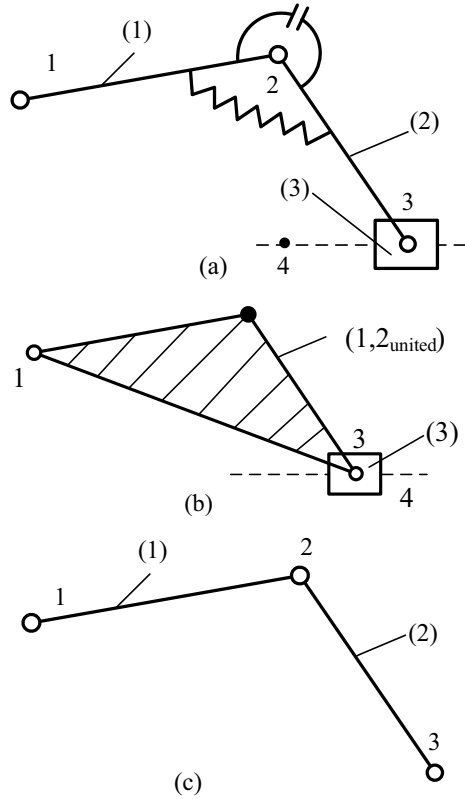
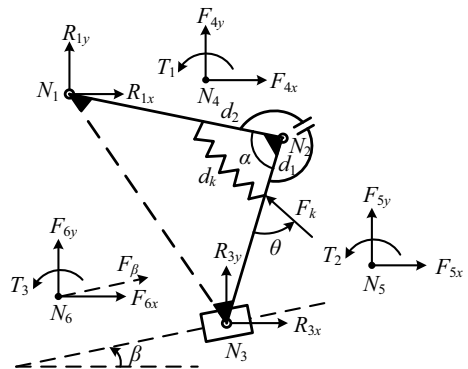


**Fig. 7** Force diagram of RRP group degraded by RRRP group



$$d_k = \sqrt{d_1^2 + d_2^2 - \frac{d_1 d_2 (l_{12}^2 + l_{23}^2 - l_{13}^2)}{l_{12} l_{23}}} \quad (2)$$

$$F_k = k(a - d_k) \quad (3)$$



$$\cos \theta = \frac{d_k^2 + d_1^2 - d_2^2}{2d_k d_1} \tag{4}$$

$$\theta = \arccos \left[ \frac{2d_1^2 - \frac{d_1 d_2 (l_{12}^2 + l_{23}^2 - d^2)}{l_{12} l_{23}}}{2\sqrt{d_1^2 + d_2^2 - \frac{d_1 d_2 (l_{12}^2 + l_{23}^2 - d^2)}{l_{12} l_{23}}} d_1} \right] \tag{5}$$

$$T_k = F_k d_1 \sin \theta \tag{6}$$

$$\begin{cases} R_{1x} = \frac{(-A_1 \sin \beta + B_1 P_{13x})}{P_{13x} \cos \beta + P_{13y} \sin \beta} \\ R_{1y} = \frac{(A_1 \cos \beta + B_1 P_{13y})}{P_{13x} \cos \beta + P_{13y} \sin \beta} \\ A_1 = -(T_{43} + T_{53} + T_1 + T_2) \\ B_1 = -(F_{4x} + F_{5x} + F_{6x}) \cos \beta - \\ (F_{4y} + F_{5y} + F_{6y}) \sin \beta \end{cases} \tag{7}$$

$$\begin{cases} R_{3x} = -(R_{1x} + F_{4x} + F_{5x}) \\ R_{3y} = -(R_{1y} + F_{4y} + F_{5y}) \end{cases} \tag{8}$$

$$F_\beta = F_{6x} \cos \beta + F_{6y} \sin \beta \tag{9}$$

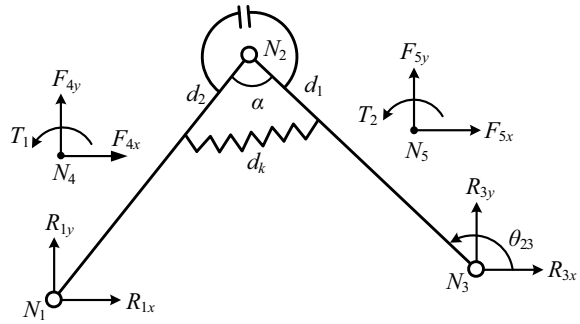
In the above equations,  $k$  denotes the spring stiffness,  $a$  denotes the original length of the spring,  $P_{ijx}$  and  $P_{ijy}$  denote the distance between point  $i$  and point  $j$  in  $x$  and  $y$  directions respectively,  $R_{ix}$  and  $R_{iy}$  denote the reaction forces of joint  $i$  in the  $x$  and  $y$  directions respectively,  $F_{ix}$  and  $F_{iy}$  denote the forces acted on point  $i$  in  $x$  and  $y$  directions respectively,  $T_{ij}$  denotes the moment of the force acted on point  $i$  to point  $j$ ,  $T_i$  denotes the moment acted on point  $i$ , and  $T_k$  denotes the moment of spring force to point  $N_2$ , that is, the constraint torque to be provided by the metamorphic joint.

$T_{42}$  and  $T_{52}$  denote the moment of the gravities of the two links  $N_1 N_2$  and  $N_2 N_3$  to point  $N_2$  respectively,  $\Delta T$  denotes the driving torque of the metamorphic revolute joint, and suppose that the counterclockwise direction is positive:

$$\begin{cases} T_{12} = P_{12x} R_{1y} - P_{12y} R_{1x} \\ T_{32} = P_{32x} R_{3y} - P_{32y} R_{3x} \\ T_{42} = P_{42x} m_{12} g \\ T_{52} = P_{52x} m_{23} g \end{cases} \tag{10}$$

$$\Delta T = T_{12} - T_{32} + T_{42} - T_{52} \tag{11}$$

**Fig. 8** Force diagram of RRR group degraded by RRRP group



In the working configuration II, the AAG RRRP degenerates into the RRR group. The force analysis of the corresponding equivalent AG RRR is shown in Fig. 8, where points  $N_4$  and  $N_5$  are the centroids of the links  $N_1N_2$  and  $N_2N_3$  respectively. Given the forces  $F_4$ ,  $F_5$  and moments  $T_1$ ,  $T_2$  acted on the links  $N_1N_2$  and  $N_2N_3$  respectively. Solve the reaction force of each revolute joint and the driving torque and constraint torque of the metamorphic revolute joint.

Modularized force analysis procedures are as follows:

$$\begin{cases} R_{3x} = \frac{(A_2 P_{32x} - B_2 P_{31x})}{P_{32x} P_{31y} - P_{32y} P_{31x}} \\ R_{3y} = \frac{(A_2 P_{32y} - B_2 P_{31y})}{P_{32x} P_{31y} - P_{32y} P_{31x}} \\ A_2 = -(T_{41} + T_{51} + T_1 + T_2) \\ B_2 = -(T_{52} + T_2 + T_k) \end{cases} \quad (12)$$

$$\begin{cases} R_{1x} = -(R_{3x} + F_{4x} + F_{5x}) \\ R_{1y} = -(R_{3y} + F_{4y} + F_{5y}) \end{cases} \quad (13)$$

$$\begin{cases} R_{2x} = -(R_{3x} + F_{5x} + F_{kx}) \\ R_{2y} = -(R_{3y} + F_{5y} + F_{ky}) \\ F_{kx} = F_k \cos(\theta_{23} + \theta - \pi) \\ F_{ky} = F_k \sin(\theta_{23} + \theta - \pi) \end{cases} \quad (14)$$

In the above equations,  $F_{kx}$  and  $F_{ky}$  denote the components of the spring force in  $x$  and  $y$  directions respectively, the calculation method of the variables  $d_k$ ,  $\theta$ ,  $F_k$ ,  $T_k$ ,  $\Delta T$  and the meaning of the other variables can refer to the force analysis in the working configuration I above.

### 3.2 Structural Design of the Metamorphic Revolute Joint

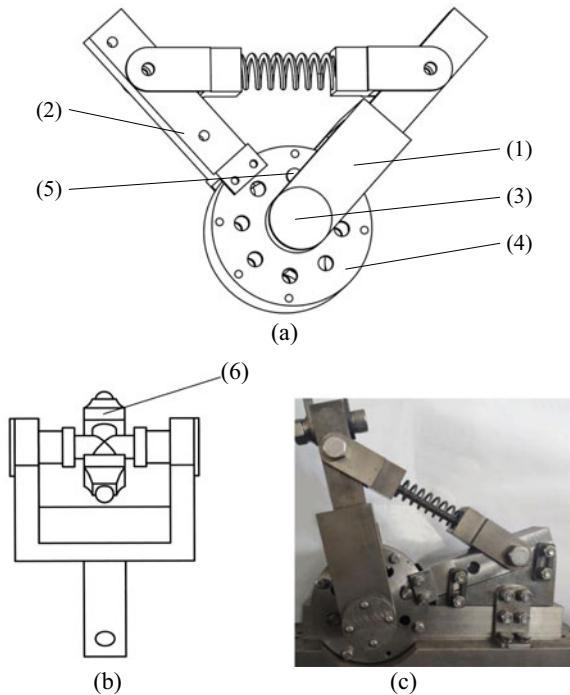
When the metamorphic revolute joint keeps static in a working configuration, the angle of its two links must be constrained neither increasing nor decreasing. The

common ways to keep static are by using spring force constraint and/or geometric constraint in the structure design of metamorphic joints. Geometric constraints can limit the increase/decrease of the angle of the metamorphic revolute joint. The spring is compressed/stretched and then installed on the metamorphic revolute joint, due to the existence of the preload, the decrease/increase of the angle of the metamorphic revolute joint is limited. The geometric constraint of the metamorphic revolute joint as shown in Fig. 8 theoretically provides infinite constraint force to ensure that the angle can't increase. At the same time, if the metamorphic revolute joint plans to keep static (the angle can't decrease) in a working configuration, the constraint torque provided by the spring force from preload should be greater than the maximum value of driving torque during the entire process of configuration keeping to limit the reduction of the angle between link (1) and (2), that is:

$$F_k \geq \frac{\Delta T}{d_1 \sin \theta} \tag{15}$$

where  $F_k$  is the spring force from preload,  $d_1$  and  $\theta$  are the corresponding structural dimensions as shown in Fig. 7. Furthermore, we can design the structural parameters of spring by using the range of spring preload calculated by Eq. (15). Therefore, a simple and practical structure of the metamorphic revolute joint was designed in this paper as shown in Fig. 9a, b, and the physical prototype is shown in Fig. 9c.

**Fig. 9** Structure of metamorphic revolute joint



As shown in Fig. 9a, b: The link (1), the end cover (3) and the component (6) are connected as a united one, the link (2) and the component (4) are connected as a united one by bolts. The balls at both ends of the component (6) can move along the grooves which are located on the internal surface of the component (4), so that the two links (4) and (6) can rotate relative to each other. As shown in Fig. 8a, the pin (5) acts as an actual geometric constraint, and the angle of this metamorphic revolute joint can't increase after the component (6) contacts the pin (5). The spring is compressed with a preload and installs on the links. When the driving torque of the metamorphic revolute joint is large enough to overcome the force of compressed spring, link (2) rotates clockwise relative to link (1) due to the release of both geometrical constraint and spring force constraint.

## 4 Design and Performance Analysis of a Multi-configurations Underactuated Constrained Metamorphic Mechanism with Variable-Constraint Constrained Revolute Joints

### 4.1 Design of a Constrained Metamorphic Mechanism with Variable-Constraint Metamorphic Revolute Joints

Figure 10 shows a 2-DOF planar constrained metamorphic mechanism, which is composed of a 0-DOF AG (RRR group) and a 1-DOF AAG (RRRP group) successively connected to the revolute driving link and the frame. The ahead RRR group reduces the maximum compression of the spring in metamorphic revolute joint  $E$ . The other spring connected to the slider makes the speed and acceleration change relatively stable during the moving process, and weakens the shock and vibration. The revolute joint  $E$  is controlled by the spring force and geometric constraints, and the prismatic joint  $F$  is controlled by the geometric constraint. The mechanism can obtain two working configurations/topological structures of the crank-slider mechanism and the crank-rocker mechanism by transforming the kinematic status of the metamorphic joints, and then complete the corresponding operation tasks in the respective configurations. The physical test bench of the mechanism is shown in Fig. 11.

The structural parameters of the mechanism are shown in Table 1, where  $l_{ij}$  is the length of the link  $ij$ ,  $m_{ij}$  is the mass of the link  $ij$ ,  $m_{\text{slider}}$  is the mass of the slider,  $J_{ij}$  is the moment of inertia of link  $ij$ ,  $\omega_1$  is the angular velocity of the driving link,  $\alpha$  is the geometric constraint angle of the metamorphic revolute joint  $E$  (the maximum angle of  $\angle CEF$ ). According to the design method in Sect. 3.2, the structure and installation parameters of the spring are determined as shown in Table 2, where  $k_1$ ,  $k_2$ ,  $a$ ,  $b$  are the stiffness and original length of spring 1 and spring 2 respectively,  $d_1$  and  $d_2$  are the distances between the installation positions of spring 1 on link  $EF$  and link  $CE$

**Fig. 10** Working-stage of the metamorphic mechanism

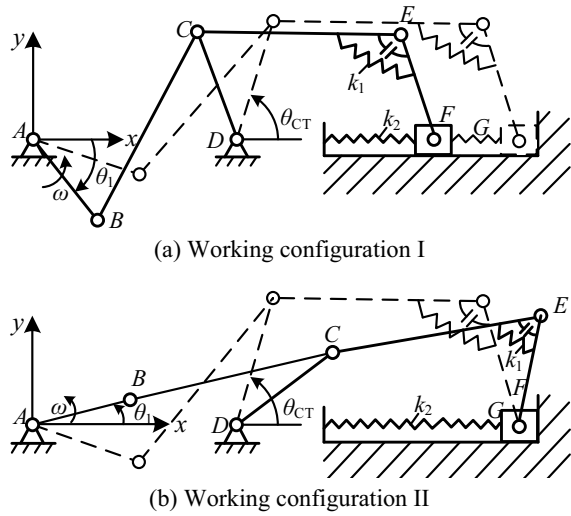


**Fig. 11** Physical drawing of the mechanism



to point *E*. According to the structure dimensions of the mechanism, the variation range of the kinematic parameters of the main links of the mechanism is determined as shown in Table 3.

**Table 1** Structural parameters of the mechanism

| Parameter                           | Value  | Parameter                | Value   |
|-------------------------------------|--------|--------------------------|---------|
| $l_{AB}/\text{mm}$                  | 180    | $l_{BC}/\text{mm}$       | 360     |
| $l_{CE}/\text{mm}$                  | 360    | $l_{EF}/\text{mm}$       | 210     |
| $l_{AF\text{-max}}/\text{mm}$       | 870    | $l_{AD}/\text{mm}$       | 315     |
| $l_{CD}/\text{mm}$                  | 240    | $m_{AB}/\text{kg}$       | 1       |
| $m_{CD}/\text{kg}$                  | 1      | $m_{CE}/\text{kg}$       | 1.5     |
| $m_{\text{slider}}/\text{kg}$       | 1      | $m_{BC}/\text{kg}$       | 1.5     |
| $m_{EF}/\text{kg}$                  | 2      | $J_{AB}/(\text{kg m}^2)$ | 0.0027  |
| $J_{CD}/(\text{kg}\cdot\text{m}^2)$ | 0.0048 | $J_{CE}/(\text{kg m}^2)$ | 0.0162  |
| $J_{BC}/(\text{kg}\cdot\text{m}^2)$ | 0.0162 | $J_{EF}/(\text{kg m}^2)$ | 0.00735 |
| $\omega_1/(\text{rad/s})$           | $2\pi$ | $\alpha/^\circ$          | 120     |

**Table 2** Spring structure and installation parameters

| Parameter           | Value | Parameter           | Value |
|---------------------|-------|---------------------|-------|
| $k_1/(\text{N/mm})$ | 10    | $k_2/(\text{N/mm})$ | 0.5   |
| $a_1/\text{mm}$     | 250   | $a_2/\text{mm}$     | 76    |
| $d_1/\text{mm}$     | 100   | $d_2/\text{mm}$     | 120   |

**Table 3** The variation ranges of some kinematic parameters

|                    | Configuration I                 | Configuration II              |
|--------------------|---------------------------------|-------------------------------|
| Type               | Crank slider                    | Crank rocker                  |
| Driving link angle | $-290.2^\circ$ to $-15.2^\circ$ | $-15.2^\circ$ to $69.8^\circ$ |
| Angle of joint $E$ | Static ( $120.3^\circ$ )        | $120.3^\circ$ to $72.5^\circ$ |
| Position of slider | 598.5 to 870 mm                 | Static (870 mm)               |
| Angle of rocker    | Static ( $115.9^\circ$ )        | $115.9^\circ$ to $88.8^\circ$ |

### 4.2 Performance Analysis of a Constrained Metamorphic Mechanism with Variable-Constraint Metamorphic Revolute Joints

Based on the theoretical calculation model, the force analysis of the paper folding mechanism were calculated by MATLAB, some calculation results are shown in Figs. 12, 13, 14, and 15. Among them, Figs. 12 and 13 shows the reaction force of kinematic joints at the fixed hinge, Fig. 14 shows the driving torque and constraint torque of the metamorphic revolute joint E in the working configuration I, and Fig. 15 shows the driving force of the metamorphic prismatic joint in the working configuration II.

It can be seen from Fig. 14 that in the entire working configuration I, the driving torque of the metamorphic joint  $E$  is less than the constraint torque provided by the spring. Therefore, the metamorphic joint  $E$  is always in a constraint status, links

**Fig. 12** The reaction force of the fixed hinges A and D in the working configuration I

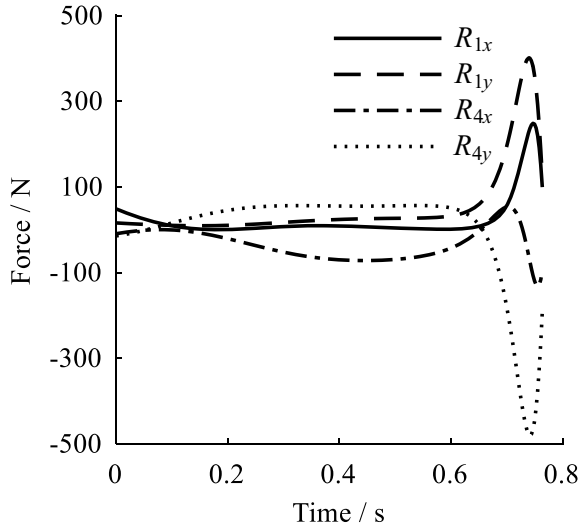
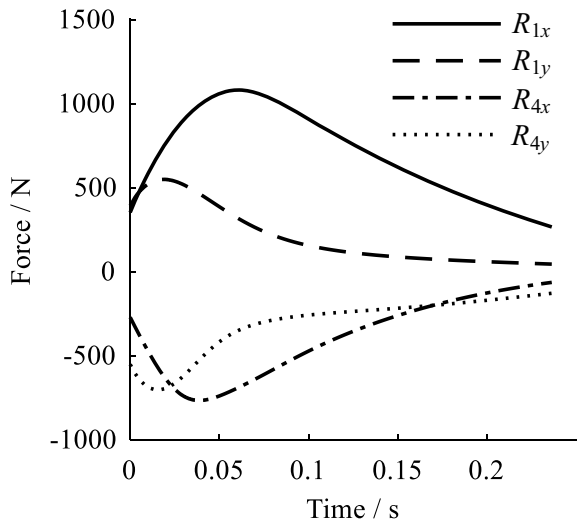


**Fig. 13** The reaction force of the fixed hinges A and D in the working configuration II



*CE* and *EF* always remain relatively static, and the mechanism is equivalent to a crank-slider mechanism. According to Fig. 15 in the entire working configuration II, the horizontal component of the reaction force on the slider is always to the right and is greater than the spring force in the left direction, so the driving force on the slider is always to the right. Due to the existence of geometric constraint, the slider is always in a constraint status, and the mechanism is equivalent to a crank-rocker mechanism.

**Fig. 14** The driving torque  $\Delta T$  and constraint torque  $T_k$  of the metamorphic revolute joint  $E$  in the working configuration I

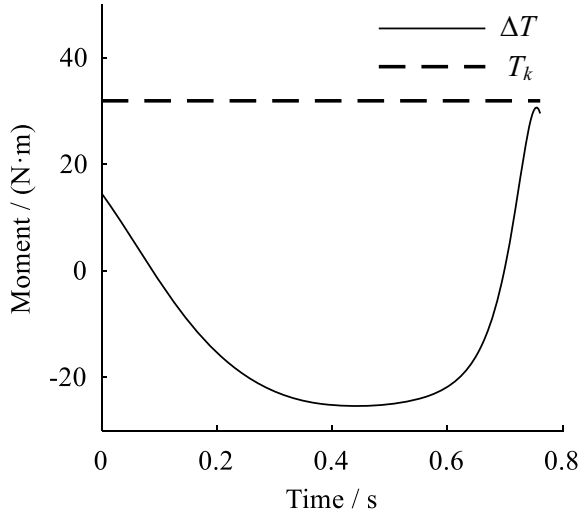
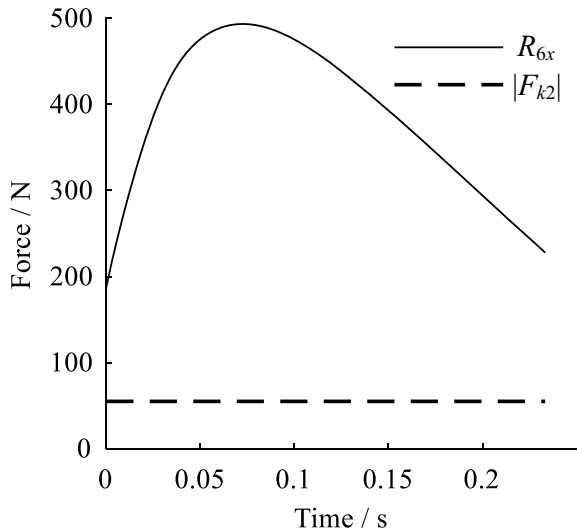


**Fig. 15** The reaction force  $R_{6x}$  and spring force  $F_{k2}$  of the slider in the working configuration II



### 5 Conclusions

According to the structure composition principle of the constrained metamorphic mechanism, the modularized force analysis models of the augmented Assur group containing metamorphic joints were established by taking the driving link, the Assur group and the augmented Assur group as basic units. According to the force analysis model, the design method of constraint parameters of the metamorphic revolute joint was proposed, and then the constraint structure of a new type of metamorphic



revolute joint with the spring force and geometric constraints was designed. As a general metamorphic functional unit for metamorphic mechanisms, this metamorphic revolute joint can provide a convenient and reliable modular metamorphic way, which contributes to rapidly construct new structures of the constrained metamorphic mechanisms. Taking a two working-configurations constrained metamorphic mechanism which contains the invented metamorphic revolute joint above as an example, the spring structure and installation parameters of the metamorphic revolute joint was designed, and the physical prototype of the mechanism was manufactured. The force analysis of the mechanism shows that this new metamorphic revolute joint can adaptively control the transformation of relative kinematic status of the two adjacent links through the change of the constraint forces generated from spring and geometric constraint, and then the configuration transformation of the metamorphic mechanism was obtained successfully. Finally, the change of the topological structure was obtained and the multi-functional operational task was realized with under-actuated. The research of this paper provides theoretical and practical references for the engineering application of constrained metamorphic mechanisms.

**Acknowledgements** Supported by National Natural Science Foundation of China (51575091), the Fundamental Research Funds for the Central Universities(N2203010), Aeronautical Science Foundation of China (20170250001).

## References

1. Dai JS, Jones JR (1999) Mobility in metamorphic mechanisms of foldable/erectable kinds. *J Mech Des* 121(3):375–382
2. Li DL, Dai JS, Zhang QX et al (2002) Structure synthesis of metamorphic mechanisms based on the configuration transformations. *Chin J Mech Eng* 038(7):12–16 (in Chinese)
3. Dai JS, Ding XL, Zou HJ (2005) Fundamentals and categorization of metamorphic mechanism. *Chin J Mech Eng* 06:7–12 (in Chinese)
4. Wang DL, Dai JS (2007) Theoretical foundation of metamorphic mechanisms and its synthesis. *J Mech Eng* 43(8):32–42 (in Chinese)
5. Li SJ, Dai JS (2012) Structure synthesis of single—driven metamorphic mechanisms based on the augmented Assur groups. *J Mech Robot* 4(3):031004-1-8
6. Zhang WX, Ding XL, Dai JS (2013) Method for configuration synthesis of metamorphic mechanisms based on constraint variation. *J Mech Eng* 49(05):1–9 (in Chinese)
7. Yang Q, Hao GB, Li SJ et al (2020) Practical structural design approach of multiconfiguration planar single-loop metamorphic mechanism with a single actuator. *Chin J Mech Eng* 33(05):29–43
8. Gan DM, Dai JS, Liao QZ (2009) Mobility change in two types of metamorphic parallel mechanisms. *J Mech Robot* 1(11):041007-1-9
9. Zhang K, Dai JS, Fang Y (2012) Geometric constraint and mobility variation of two 3SvPSv metamorphic parallel mechanisms. *ASME J Mech Des* 135(1):011001, January 2013
10. Zhao C, Guo H, Liu R, Deng Z, Li B (2018) Design and kinematic analysis of a 3RRIS metamorphic parallel mechanism for large-scale reconfigurable space multifingered hand. *ASME J Mech Robot* 10(4):041012
11. Wang R, Kang X, Dai JS (2021) A novel reconfigurable spherical joint based on linear independence of screws and its resultant metamorphic mechanisms. *Mech Mach Theory* 164:104351, ISSN 0094-114X

12. Jiangnan L, Wenbo Z (2017) Study on design catalogue of variable joints of variable topology mechanism. *J Hunan Univ (Nat Sci)* 44(10):33–40
13. Yan H, Kuo C (2005) Topological representations and characteristics of variable kinematic joints. *ASME J Mech Des* 128(2):384–391
14. Li SJ, Wang HG, Yang Q (2015) Constraint force analysis of metamorphic joints based on the augmented Assur groups. *Chin J Mech Eng* 28(04):747–755
15. Simionescu P (2019) Kinematics of the RRR, RRT (passive) and RRRR, RRRT (active) linkage-mechanism building blocks with applications and reporting of new findings. *J Mech Robot* 11(6):1–24